Jordan Journal of Civil Engineering, Volume **9**, No. **3**, **2015**

Prediction of Mechanical Properties of Reactive Powder Concrete by Using Artificial Neural Network and Regression Technique after the Exposure to Fire Flame

Mohammed Kadhum

College of Engineering, Babylon University, Iraq
E-Mail: moh_alkafaji@yahoo.com

ABSTRACT

An experimental work was carried out to investigate some mechanical properties of Reactive Powder Concrete (RPC) which are particularly required as input data for structural design. These properties include compressive strength, flexural strength, tensile strength and static modulus of elasticity. A combined laboratory and modeling study was undertaken to develop a database of the estimation ability of the effects of exposure to real fire flame on the mechanical properties of reactive powder concrete using 2 different models: artificial neural network (ANN) and regression techniques. Experimental results were used in the estimation models. After being subjected to high temperatures from 200 to 500°C, the residual mechanical properties were determined, and RPC was considerably spalled under high temperature. Exposing to high temperatures from 200 to 400°C, mechanical properties were enhanced more or less, which can be attributed to further hydration of cementitious materials activated by elevated temperature. It was found that RPC can be used at elevated temperatures up to 300°C for heating times up to 1 hour, taking into consideration the loss of strength. Finally, prediction performances of reactive powder concrete single and multiple variable regression equations were developed, and ANN was compared. According to this comparison, best prediction performance which belongs to ANN was improved.

KEYWORDS: Reactive powder concrete, Fire flame, Artificial neural network, Mechanical properties, Statistical analysis.

INTRODUCTION

Reactive powder concrete (RPC) is one of the latest advances in concrete technology. It addresses the shortcomings of many concretes today (Therresa et al., 2008). RPC has attracted great research attention for its ultrahigh strength and high durability (Cheyrezy et al., 1995; Bonneau et al., 1996). It represents a special concrete wherein the microstructure is optimized by precise gradation of all particles in the mix to yield maximum density (Sujatha et al., 2014).

RPC can be used in various applications, such as prestressed concrete structures, nuclear power stations, large-span arch-roof structures and bridges. Fire is still a potential risk. However, so far there are only a few reports on fire resistance or fire behavior of RPC, and experimental data are especially lacked for evaluating fire resistance of RPC (Hassan, 2012). Since 2000, a couple of investigations by means of computer modeling revealed that RPC is prone to explosive spalling under high temperature (Schneider et al., 2003; Ratvio, 2001). Moreover, an experimental investigation

Accepted for Publication on 3/3/2015.

in 2009 found that RPC spalled under high temperature, in a manner as layer by layer when column specimens were used, which was quite different from that of high-strength or high-performance concrete reported in most literature (Liu and Huang, 2009). A sudden exposure of RPC to high temperature may lead to the spalling occurrence; this was proven to be most likely due to the internal gas pore pressure increase during heating (Hagera et al., 2013). But the mechanism for spalling behavior of RPC remains unknown. Furthermore, mechanical properties including strength and fracture energy of RPC exposed to high temperature are also of great concern.

The fire performance of RPC is of importance and necessitates investigation prior to proper usage in construction industries using Artificial Neutral Network (ANN) and RT. Liu and Huang (2009) conducted a series of fire resistance tests and found that the residual compressive strength of RPC decreases with the increase in fire duration.

Recent studies have been performed on the usability of ANN in civil engineering related problems, especially in areas of concrete technology (Subasi and Beycioglu, 2008; Sancak, 2009). The use of ANN is to get information about the relative importance of factors affecting the predicted engineering properties of RPC before and after burning. Moreover, ANN can be used as there are flexible and complex relationships between inputs and outputs discovered by changing the model structure and the connection weights (Ozer et al., 2008). Previous studies indicated a reliable predictive tendency of ANN (Lee, 2003) in concrete compressive strength determination. Topcu and Saridemir (2008) utilized ANN and Fuzzy Logic for the determination of compressive strength of fly ash added concretes. They concluded that both ANN and Fuzzy Logic methods have high predictive performance. Altun et al. (2008) used ANN and multiple linear regression techniques for the estimation of compressive strength of steel fiber reinforced concrete. Subasi (2009) developed ANN for the estimation of mechanical properties of fly ash added cement paste and concluded that ANN has a better performance than multiple linear regression technique.

MODELLING APPROACHES

The modeling approaches used for this study are briefly described below.

A. Regression Technique

Regression technique (RT) is the modeling of the relationship between one or more measured variables and another variable which is genuinely considered to be related to the measured variable(s). In this technique, the influencing variable, that is, the variable that causes an apparent change in the other variable is called the explanatory variable (or independent variable) and the variable which is influenced by the independent variable, that is, the variable affected by the apparent change caused by the independent variable is called-dependent variable (Kalayci, 2006). Regression models can be classified as linear and non-linear models. However, non-linear models can be transformed into linear models by various methods. To make a good prediction with non-linear regression models, you have to possess preliminary information on the assumed degree of the model. The formulation of the equations of multiple linear regression is given in Equation 1.

$$Y = b_o + b_1X_1 + \cdots + b_nX_n + \varepsilon \quad (1)$$

In the model equation,
Y = Dependent variable;
X_i = Independent variable;
b_i = Calculated coefficient parameters;
ε = Error term.

B. Artificial Neural Networks

Over the decades, artificial neural networks technology, a sub-field of artificial intelligence, has been used to solve a wide variety of problems in civil

engineering applications (Adhikary and Mutsuyoshi, 2006; Pala et al., 2007; Topcu and Sarıdemir, 2008). The most important property of ANN in civil engineering problems is their capability of learning directly from examples. The other important properties of ANN are their correct or nearly correct responses to incomplete tasks, their extraction of information from noisy or poor data and their production of generalized results from the novel cases. The above-mentioned capabilities make ANN a very powerful tool to solve many civil engineering problems, particularly problems where available data is complex or limited (Ince, 2004).

A typical ANN model is a combination of layers made of neurons. The most widely used ANN type is the multi-layer type (MLP). MLP primarily consists of an input layer that takes in the data, an output layer that conveys the output of the network out and usually a hidden layer in between these layer. The input of the neurons is taken in from outside. Nevertheless, the net input of a neuron in the hidden layers or the output layer is the sum of multiplications of all the inputs received (x_i, i = 1, 2,..., n) by the corresponding weights (w_i, i = 1, 2,.., n), that is, ($\sum_i w_i.x_i$), while the output of a neuron is obtained after the net input is processed by the activation function (Lin and Lee, 1996; Zhang et al., 1998). As shown in Fig.1, a typical neural network showing the aforementioned layers is built to determine the relationship between the independent variables (input) and the dependent variables (output). Numeric value for the output of a neuron is calculated using Equation 2. In Fig. 1, Equation 2 is used.

$$O = f\left(\sum_{i=1}^{n} w_i\, x_i + b\right) \qquad (2)$$

where n is the number of input nodes, f is the activation function, x_i is i^{th} (i = 1 to n) input variable, w_i represents the weights for input nodes and b is the weight of the arc leading from the bias term whose value is equal to 1 (Hamzaçebi and Kutay, 2005).

Research Significance

In this study, an experimental investigation was conducted on explosive spalling and mechanical properties of RPC subjected to high temperature. The parametric variables in this study are; age, density, fire flame temperature and type of cooling. The significance of this study lies in that it leads to know the behavioural pattern of RPC under the influence of extreme fire condition with the aim of determining its suitability in precast concrete elements at elevated temperature. Similarly, the study will provide essential information on the influence of extreme fire temperatures on RPC. Hence, in this study, artificial neural networks and regression techniques were used for the prediction of compressive, splitting and flexural strengths as well as modulus of elasticity of RPC after exposure to real fire flame.

EXPERIMENTAL SET-UP

All tests in this research were carried out in the Construction Materials Laboratory at Civil Engineering Department, Faculty of Engineering, Babylon University, Iraq. Materials used, preparation, casting, curing of test specimens and test procedure are discussed in this section.

Materials

The RPC is prepared using: Ordinary Portland cement (OPC) manufactured by a united cement company commercially known as TASLUJA-BAZIAN. The chemical constituents passed the Iraqi specification requirement (IQS No.5/1984). Similarly, the chemical and physical compositions are in accordance with ASTM C120 specification. The chemical composition and specific surface of cement and silica fume are presented in Table 1. In this table, L.O.I represents loss on ignition; I.R represents insoluble residue and L.S.F represents lime saturation factor. Al-Ukhaider natural sand of maximum size of 600 μm was used. Its gradation lies in zone (4). The gradation and sulfate content results of fine aggregate were within the requirements of the Iraqi specification No. 45. Table 2 shows the gradation properties of the

sand used in the study. Potable water was used for both mixing and curing of test specimens. Brass-coated steel micro-fibers (13 mm long and 0.18 mm in diameter, tensile strength greater than 2500 MPa) were used throughout the experimental program. Additionally, an attempt was made to improve slurry at low water-cement ratios by using a high performance water-reducing agent. It represented aqueous solution of modified polycarboxylate - based super plasticizer (SP) SikaViscocrete-5930. Table 3 shows that SikaViscocrete-5930 is free of chlorides and complies with ASTM C494-99 type G and F specifications.

Table 1. Cement and silica fume chemical composition and specific surface value

Materials	CaO	SiO_2	Al_2O_3	Fe_2O_3	SO_3	MgO	Alkalis	L.O.I	I.R	L.S.F	Fineness m^2/kg
OPC	62.21	19.88	4.89	3.47	2.48	2.46	1.15	3.30	1.29	0.95	345
Silica Fume	0.40	94.85	0.54	0.06	0.12	0.20	0.41	2.80	-	-	19880

Table 2. Fine aggregate properties

Sieve Size [mm]	Cumulative Passing %	Limits of Iraqi Specification No.45/1984, Zone 4
4.75	100	90-100
2.36	100	95-100
1.18	100	90-100
0.600	100	80-100
0.300	44	15-50
0.150	7	0-15
Fineness modulus= 1.5		
Specific gravity= 2.69		
Sulfate content =0.12% (Iraqi specification requirement ≤ 0.5%)		
Absorption = 0.72%		

Table 3. Sika viscocrete-5930 properties

Basis	Aqueous Solution of Modified Polycarboxylate
Boiling	100°C
Odor	None
Appearance	Turbid liquid
Color	Turbid liquid
Specific gravity	1.08 kg/It. ± 0.005
pH	7-9
Chloride content	None
Toxicity	Non-Toxic under relevant health and safety codes.
Storage	Protected from direct sunlight and frost at temperatures between + 5°C and + 35°C.

Mixture Proportions

The mix ratios are based on guidelines given in previous studies (Hassan, 2012; Hussein, 2011). The materials making up the RPC were as follows: 910 kg/m^3 of OPC; 230 $kg/m^3$of silica fume; 960 kg/m^3 of natural sand; steel fibers content of 40 kg/m^3, super plasticizer of 36.4 kg/m^3, and the water-binder ratio was 0.17.

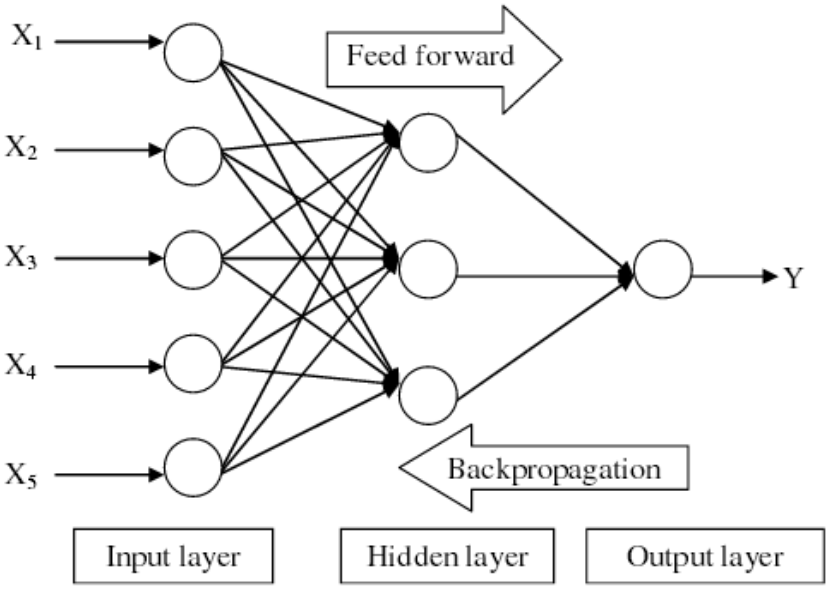

Figure (1): Architecture of a typical multi-layer feed forward neural network

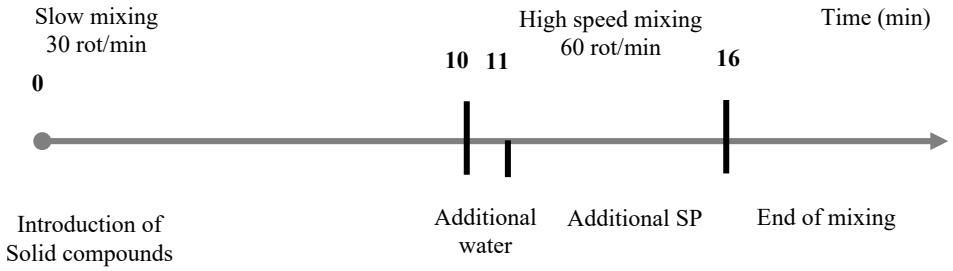

Figure (2): **Mixing procedure of RPC**

Mixing Procedure

All trial mixes were performed in a small rotary mixer of 0.01m^3 capacity, while mass production of RPC specimens was performed in a rotary mixer of 0.09m^3 capacity. Before using the mixer, any remaining concrete from the previous batch was cleaned off. A damp cloth was used to wipe the pan and the blades of the mixer. The silica fume powder was mixed in dry state with the required quantity of cement for five minutes to ensure uniform dispersion of the reactive powder particles throughout the cement particles. Then, fine sand was added and mixed for five minutes. Additional tap water was added to the rotary mixer within one minute. Then, all the super plasticizers were added and mixed for additional five minutes. When steel fibers were used, they were introduced and dispersed uniformly. Then, these were added slowly to the rotary mixer after the rest of the materials had been properly mixed and the concrete had a wet appearance and mixed for additional two minutes. The procedure shown in Fig. 2, was rigorously applied for each batch. Mixing one batch

required approximately twenty minutes from adding water to the mix.

Casting Procedure

Before casting, all molds were well cleaned and their internal surfaces were lightly oiled to avoid the adhesion of hardened concrete to them. The molds were filled with the concrete mix in layers. Each layer was compacted by a tamping rod to minimize the air voids and to achieve proper compactness. The top surfaces of the molds were leveled, and the specimens were covered with polythene sheets, then put in a wetting room to minimize moisture loss and shrinkage effect. After twenty-four hours, the specimens were demolded and marked for curing in a normal water tank (23±2 °C) until the day of test.

Burning Temperature and Testing Methodology

Three specimens representing same constituents were used for each test throughout this study, and the average values were reported. At ages of 3, 7, 28, 56 and 90 days, a control set of unheated specimens is tested for mechanical and physical properties of RPC and the other specimens were burnt in a brick stove to a target temperature of between 200-500°C (100°C increment), as shown in Fig. 3. After the exposure to the target temperature, the fire flame was switched off at the end of the exposure time. The specimens were removed immediately after being extinguished and picked up by a steel frame. Two methods were used to cool the specimens: after being exposed to direct fire flame, cooling by air method was used. The second one is the common cooling method in which the modern extinguishing way is used. The two methods represent a simulation to practical reality. For each data point of the test, three identical specimens were used to ensure repetition in all tests.

The specimens were burnt with direct fire flame from a net of methane burners inside a brick stove with dimensions of 1500×1500×800 mm. The bare flame was intended to simulate the heating condition in an actual fire. The intensity of the flame was adjusted to raise the specimens to different temperatures. When the target temperature was reached, the temperatures were continuously recorded at different depths by applying an infrared ray thermometer approximately two meters from the concrete exposed to fire.

Figure (3): Brick stove of net methane burner

Three specimens representing same constituents were used for each test throughout this study and the average values were reported. All tests in this research were carried out to investigate the main properties of RPC samples which are reported in this section.

- Explosive Spalling and Compression Test: Cube specimens of dimensions 50×50×50 mm, were prepared for evaluating the explosive spalling and compressive strength, and the test was carried out according to BS: 1881: part 116. A 2000 kN capacity compression testing machine was used.
- Tension Test: Cylindrical concrete specimens, having a diameter of 100 mm and 200 mm high, are prepared to evaluate the tensile strength depending on ASTM C496-05 specification. Indirect tension test (splitting method) was performed to determine the tensile strength of concrete mixes. A 2000 kN capacity compression testing machine was used.
- Flexural Strength Test: This test was performed

according to the ASTM C 78-02 standard by using prisms of 50×50×300 mm. Each prism was simply supported and subjected to a two-point loading using an electrical testing machine with a capacity of 2000 kN (loading rate: 0.2 mm/min for fiber reinforced RPC).

- Modulus of Elasticity Test: This test was carried out on cylindrical specimens with dimensions of 100 mm diameter and 200 mm height. The 40% of ultimate compressive strength of concrete specimen was applied on the concrete cylinders to perform the elastic modulus test as specified by ASTM C-469-02. A 2000 kN capacity compression testing machine was used to apply a compressive axial load and a compress meter (dial gauge with an accuracy of 0.01 mm and a maximum capacity of 10 mm) was used.

RESULTS AND DISCUSSION

Mechanical Properties

Explosive Spalling

The spalling mechanism is the change of reactive powder concrete specimens under high temperature exceeding (500ºC) of concrete under fire or otherwise may be included as follows:

Sequence of Spalling

Sounds were recorded for RPC specimens after exposure to high temperature. By analyzing the results before and after the spalling, sequence was observed at temperatures around (500 ºC) in cases where spalling took place.

1. During 3-5 minutes, sound of crack propagation was heard;
2. Small pieces fell out of the surface layer;
3. After spalling, big parts fell out;
4. After completing one hour and removing the fire source, the specimens were characterized by different shapes and edge damage.

Thus the above behavior of RPC specimens may be due to internal cracks. Internal cracking took place prior to explosive spalling. According to Phan et al. (2001), explosive spalling of high strength concrete (HSC) occurs in the temperature range between 300 and 650°C. However, a value of about 450°C is recorded in this study using RPC. Several factors are identified to influence explosive spalling, such as age, moisture content, type of gravel and sand used, curing method and rate of heating.

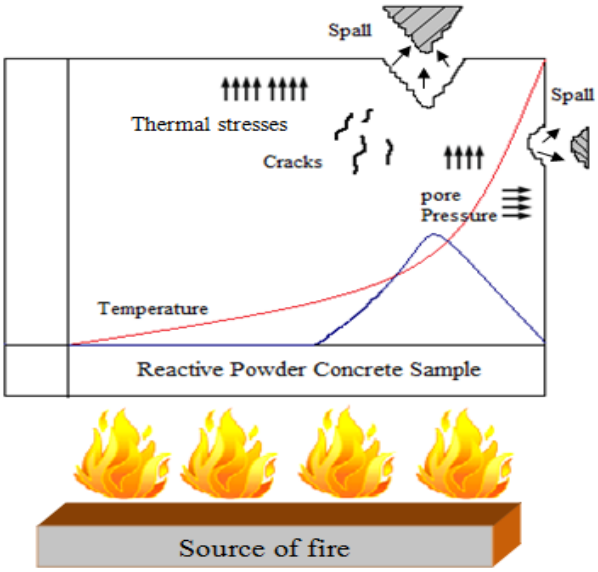

Figure (4): Suggested mechanism of spalling of RPC specimens under burning by real fire flame

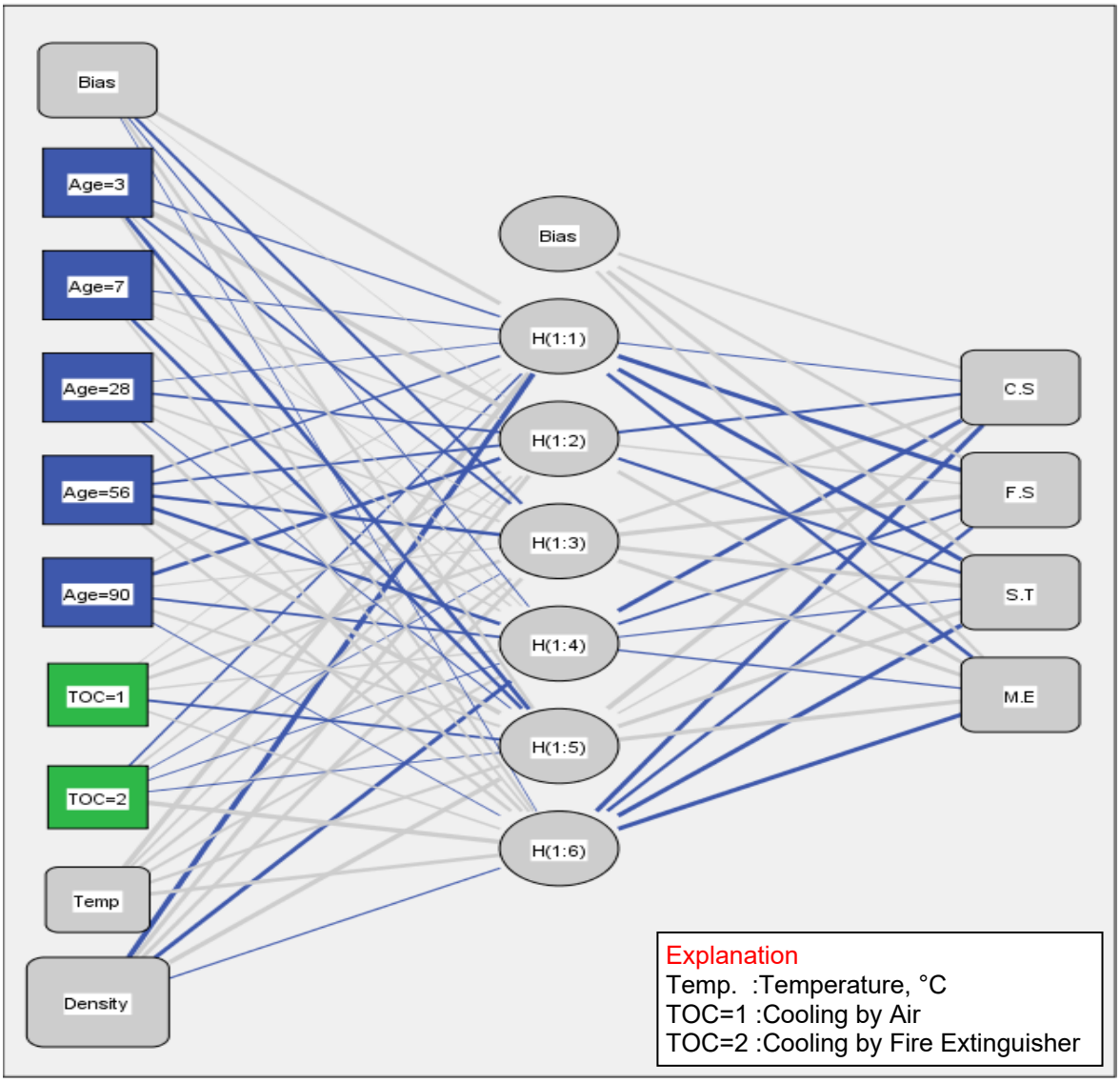

Figure (5): Structure of the neural network for prediction of mechanical properties of RPC

Suggested Mechanism of Spalling

By summarizing the results from fire tests and depending on images taken for the specimens during and after exposure to real fire flame, the main reason behind spalling was internal cracks. Partial or total splitting of surface layer from different depths beneath the core of specimen was suspicious considering that there is no significant damage on the surface. As explained in the prior paragraph, pullout of some parts from the surface occurred before the cracking took place. This may not be unconnected with spalling, because of split layer buckling. Similarly, pore pressure rise might have contributed to spalling. This behavior is clearly illustrated in Fig.4.

Strength Test

The results of compressive strength, tensile splitting strength and flexural strength of RPC before and after exposure to fire flame are given in Table 4. The

Table 4. Test values of engineering properties of RPC specimens before and after burning

Age at Exposure (days)	Temperature [ºC]	Density [gm/cm^3]	Compressive strength [MPa]	Flexural strength [MPa]	Splitting strength [MPa]	Modulus of elasticity [MPa]	Type of Cooling
3	23	2.48	91.12	30.00	9.90	37.07	Air
	200	2.48	100.38	39.60	12.70	39.66	
		2.48	94.80	38.28	11.35	37.81	Extinguisher
	300	2.36	66.69	21.60	6.63	26.32	Air
		2.38	65.52	21.00	6.24	24.84	Extinguisher
	400	2.31	61.05	19.50	6.14	23.72	Air
		2.33	59.23	18.60	5.94	22.61	Extinguisher
7	23	2.49	99.40	33.64	13.42	37.70	Air
	200	2.49	123.00	42.24	14.41	42.22	
		2.52	109.00	40.09	14.19	41.09	Extinguisher
	300	2.39	79.02	25.57	9.25	27.52	Air
		2.42	76.74	24.56	8.59	26.39	Extinguisher
	400	2.35	72.57	23.21	8.86	25.26	Air
		2.37	70.28	22.54	8.32	24.13	Extinguisher
28	23	2.50	132.30	35.40	15.67	41.00	Air
	200	2.55	143.80	47.50	16.72	47.15	
		2.60	134.70	45.24	16.50	45.51	Extinguisher
	300	2.42	102.22	27.26	11.59	30.75	Air
		2.43	100.24	26.19	10.97	29.11	Extinguisher
	400	2.38	91.24	25.84	11.28	29.52	Air
		2.38	88.78	24.78	10.65	28.29	Extinguisher
56	23	2.51	147.50	36.90	16.00	46.00	Air
	200	2.62	157.20	49.40	17.50	54.74	
		2.69	154.20	47.14	16.90	52.44	Extinguisher
	300	2.45	126.99	30.26	12.48	35.88	Air
		2.46	125.67	29.52	11.84	34.50	Extinguisher
	400	2.43	112.10	27.68	11.84	34.04	Air
		2.44	109.29	26.19	11.20	32.66	Extinguisher
90	23	2.56	174.05	43.54	18.88	54.28	Air
	200	2.67	185.50	58.29	20.65	64.59	
		2.74	181.96	55.63	19.94	61.88	Extinguisher
	300	2.50	149.85	35.71	14.73	42.34	Air
		2.50	148.29	34.83	13.97	40.71	Extinguisher
	400	2.48	132.28	32.66	13.97	40.17	Air
		2.49	128.96	30.90	13.22	38.54	Extinguisher

recorded results showed that the compressive strength values of RPC increase with the rise in temperature up to 200°C then drop afterwards with further increase in temperature, as demonstrated in this study. This behavior is in agreement with a study conducted by Toumi et al. (2009), while strength values of other specimens drop at target temperature. Meanwhile, as temperature increased from 23 to 200°C, an internal autoclaving for RPC occurred. This in turn led to further hydration of cement with silica fume as a

pozzolanic reaction. Consequently, this reaction resulted in increasing the hydration products and reducing the pore size. Also, silica fume can react with calcium hydroxide released from cement hydration to perform calcium silicate hydrates (C-S-H). The chemical reaction, leading to improve compressive strength, reduces micro-cracking, reduces voids and strengthens the micro-structure. Chemical changes lead to an increase in the compressive strength at this range of temperature. Test results indicated also that if the fire temperature increases up to 400°C, there is a remarkable decrease of compressive strength. When the compressive strength before burning is in the range of (175 MPa) at the age of 90 days, the percentage residual compressive strength after exposure to (300 and 400°C) is about (86% and 75%), respectively. The specimen exploded at an operational temperature of 500°C. At this range of temperature, the absorbed water and poured water were gradually directed to be lost. The decarbonation of calcium carbonate and dehydration of C-S-H produced a weak structure. Additionally, water loss increases the number of pores in the tested specimens structures. All these factors contributed to the reduction of compressive strength value.

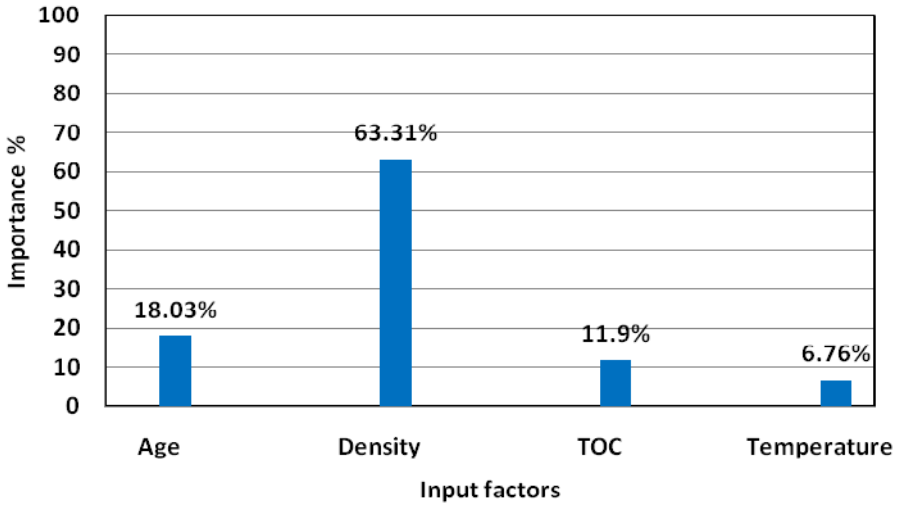

Figure (6): Relative importance of input parameters for the prediction of engineering properties of RPC

The loss in tensile splitting strength was considerable at the range 200-500°C, which was clearly different from the change in compressive strength, which increased in the range 23-200°C and then gradually decreased in the range 200-500°C. This happened because tensile strength is more sensitive to flaws either on macro- or micro-scale which were caused by high temperatures of concrete (Chan et al., 1999). It is also possible that the different rates of cooling between the surface and the inner part of the specimens caused an increase in the amount and volume of cracks and ultimately lowered the tensile strength.

It is clear from the test results that the higher reduction in mechanical properties of RPC occurred in the modulus of rupture when exposed to fire flame at 400°C. These results can be attributed to the higher sensitivity to the loss of moisture content of modulus of rupture compared with that of other mechanical properties, where the drying of the specimen results in a reduction in the measured modulus of rupture. Their flexural strength increased when specimens were burnt at 200ºC and then decreased with further increase in temperature. The strength increase can be attributed to

the increase in bonding force due to further hydration of cement paste. The decrease can be attributed to thermal cracking, formation of interconnected pores and pore structure coarsening. From Table 4, it can be seen that mechanical properties values for specimens cooled in the fire extinguisher were lower compared with air cooled specimens. This may be due to thermal choke in case of rapid cooling, where a difference in temperature occurred between the surface and the core of the specimens and led to an internal change in the microstructure of the RPC specimens.

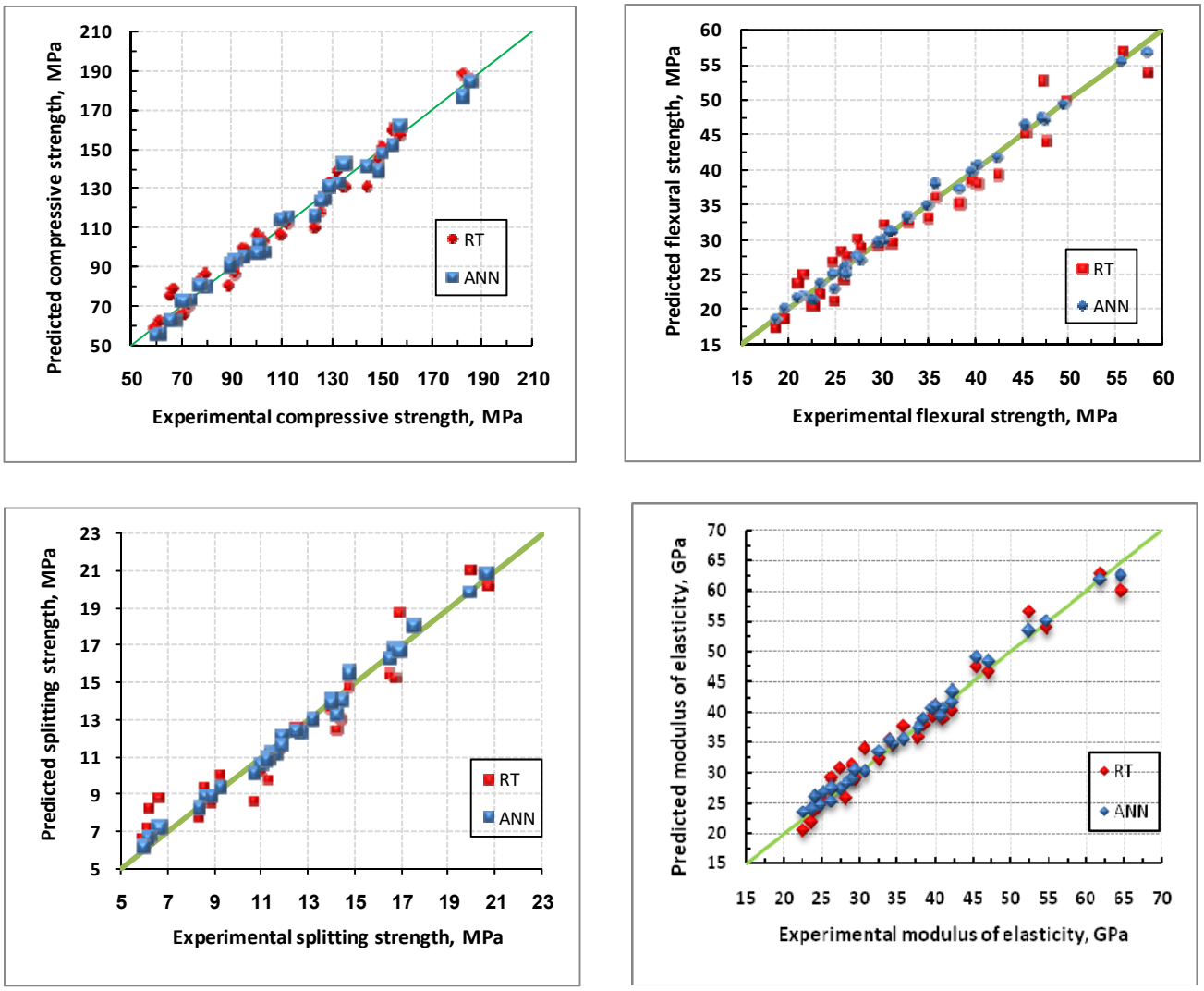

Figure (7): Performance comparison of observed values with predicted values obtained from ANN and RT models of RPC after burning

Static Modulus of Elasticity Test

The test results of the modulus of elasticity of RPC before and after exposure to fire flame are presented in Table 4. The results show that the decrease in modulus of elasticity values of RPC is more significant than in compressive strength at identical fire flame temperatures. The reductions in modulus of elasticity after exposure to fire temperature (300 and 400°C)

were (25-33%) and (29-39%), respectively, while the reductions in compressive strength were (14.8-28%) and (25.8-34.8%) at the same temperature. The reduction in the modulus of elasticity was due to the breakage of bonds in the micro-structure of the cement paste and the differential movement between the cement paste and the aggregate, which took place when the RPC was subjected to high temperatures of firing process.

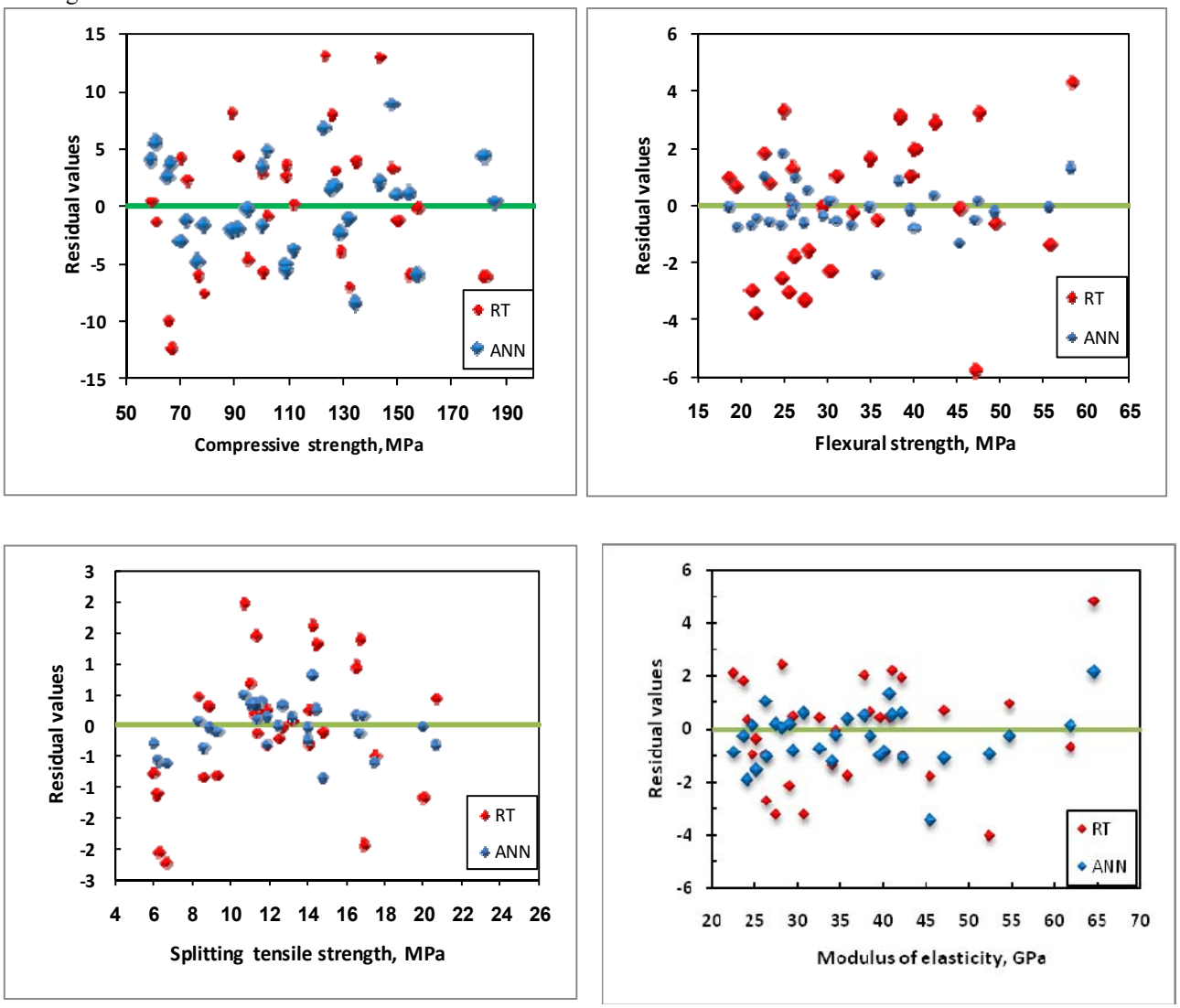

Figure (8): The distribution of the residual values with predicted values of RPC after burning for ANN and RT models

From the recordes results, it was apparent that the bulk values of the modulus of elasticity occur between the temperatures of 23 to 200 ºC. When the temperatures change (23 to 200ºC), an expected pozzolanic reaction between cement and silica fume occurs. This level of temperature showed a higher modulus value than its value in the laboratory and other temperature levels. This led to further hydration and increased the hydration products and reduced the pore size. This may lead to increase the strain of reactive

powder concrete specimens with respect to stress increase. At 300 ºC, there was a significant reduction in the modulus of elasticity due to the effect of fire flame. The residual modulus of elasticity ranged between 71-78% and 67-75% for specimens cooled by air and fire extinguisher, respectively. At 400 ºC, there was a sharp

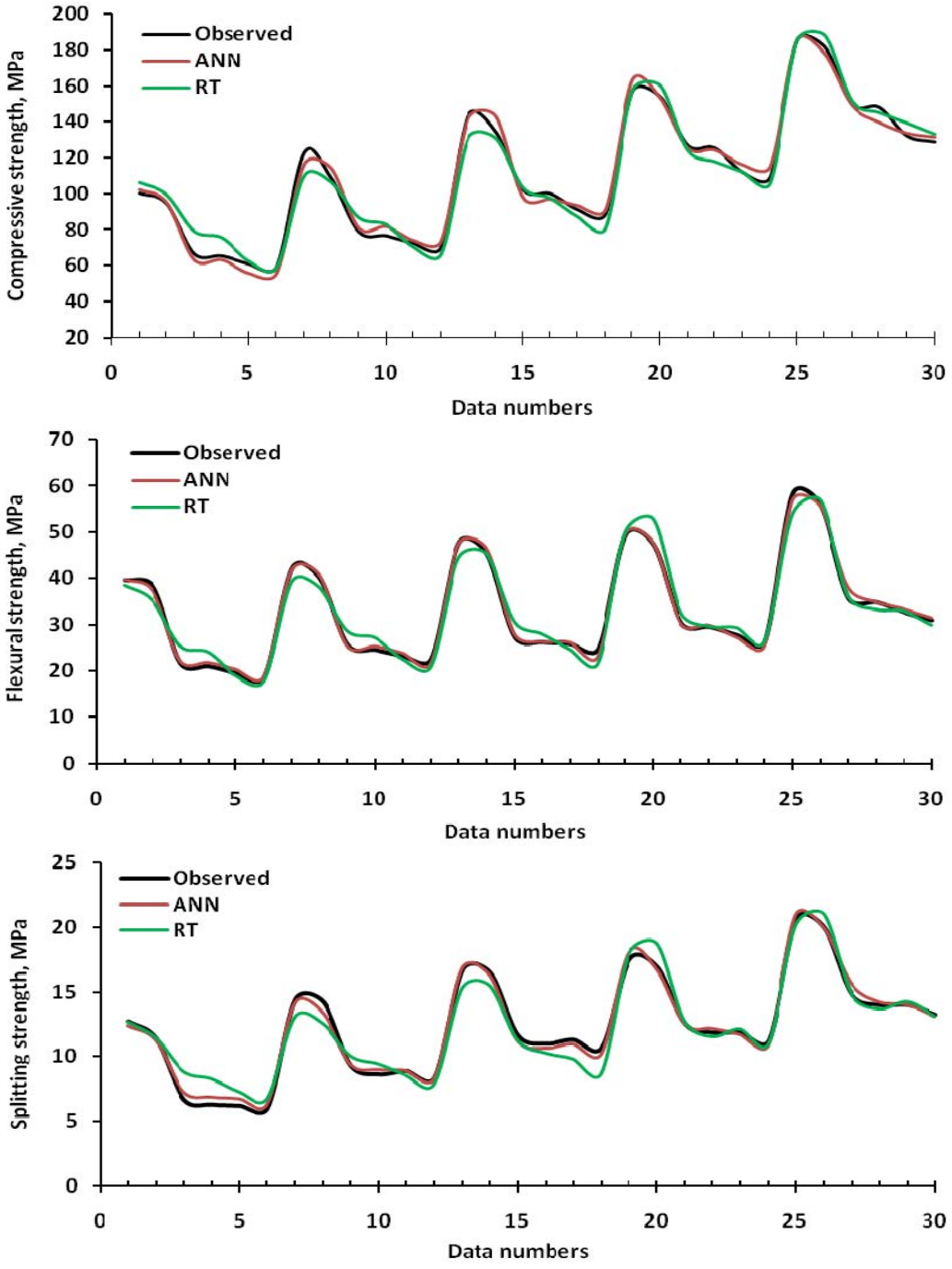

Figure (9): Comparison of predicated values and observed values of RPC strengths for ANN and RT

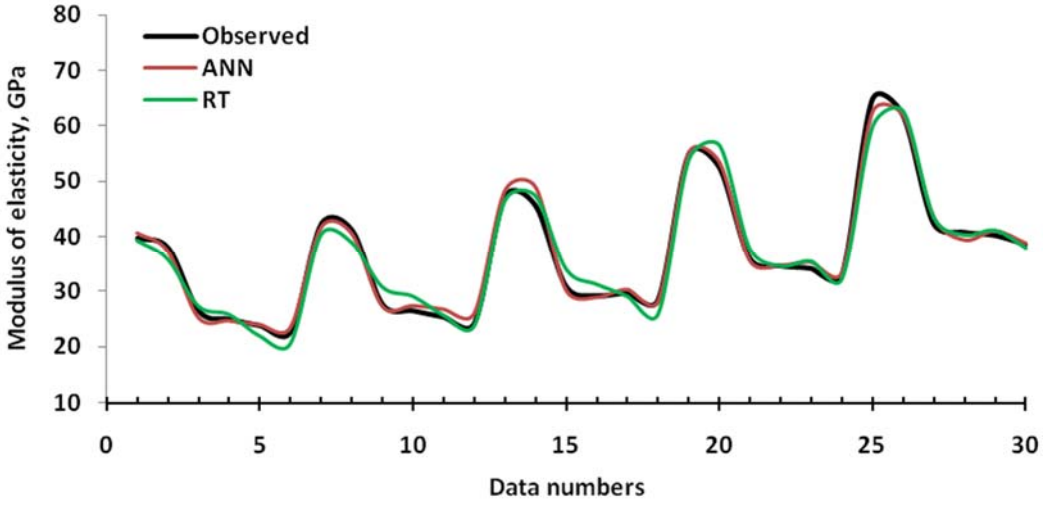

Figure (10): Comparison of predicated values and observed values of modulus of elasticity of RPC for ANN and RT

Table 5. Range of input and output parameters used in database

Input variables	Data used in training and testing the models	
	Minimum	Maximum
Age of specimen (day)	3	90
Density, gm/cm^3	2.31	2.74
Temperature, °C	23	400
Type of cooling	--	
Compressive strength, MPa	59	185
Flexural strength, MPa	18	58.29
Splitting strength, MPa	5.94	20.65
Modulus of elasticity, GPa	22.61	64.59

Table 6. The equations of multiple linear regression models

Experiment	Regression coefficient R^2	Model equations $Y = a+bX_1+cX_2+dX_3$
Compressive strength	0.952	C.S= -213.01+0.601Age-0.098Temp-6.952TOC-138.645Density
Flexural strength	0.944	F.S= -180.22-0.0235Age-0.0193Temp-3.496TOC+91.18Density
Splitting tensile strength	0.925	S.T= -61.52+0.0189Age-0.0008Temp-1.299TOC+30.49Density
Modulus of elasticity	0.951	M.E= -176.79+0.039Age-0.009Temp-3.621TOC+89.26Density

reduction in E_c values for both types of cooling and the residual modulus of elasticity was between 64-74% and 61-71% for respective specimens. Modulus of elasticity showed a difference in results between specimens cooled by air and others cooled by fire extinguisher. This clearly shows the difference between the cooling methods adopted in this study. Evidently, there is a marginal gain of about 3-5% in air cooled specimens over the extinguisher ones.

Prediction with RT

Linear regression model was used in the prediction of compressive strength, flexural strength, splitting tensile strength and modulus of elasticity of RPC after burning. Non-linear regression model was not preferred here as there was no information about the data structure. Since the degree of the non-linear regression model was unknown previously, this necessitated the use of the linear regression model. In the formulated model, the independent variables were: specimen age, density, fire temperature and cooling method; whereas the dependent variables were the mechanical properties. A total of 25 data were used in forming the regression model and five data were used in testing the model equation obtained. The limit values of variables used in the multiple linear regression models were listed in Table 5. The prediction model used in this study is shown in Equation 3. Where X_1 is the age of specimen, X_2 is the temperature level, X_3 is the type of cooling and X_4 is the density of the specimens, the equations with the coefficients obtained from multiple linear regression analysis are given in Table 6.

$$\text{Engineering properties} = b_1 X_1 + b_2 X_2 + b_3 X_3 + b_4 X_4 \quad (3)$$

Table 7. The prediction performances of both techniques for the testing set

Prediction models	Compressive strength		Flexural strength		Splitting strength		Modulus of elasticity	
	ANN	RT	ANN	RT	ANN	RT	ANN	RT
RMSE	4.020	6.090	0.820	2.370	0.380	1.040	1.100	1.940
MAPE	0.3340	0.7013	0.6275	0.6270	0.0287	0.0747	0.0233	0.0433
MPA	-0.0031	0.7013	0.6275	0.6270	0.0046	0.0040	0.0103	0.0030
R^2	0.987	0.952	0.994	0.948	0.990	0.925	0.989	0.951
AA	0.9666	0.2987	0.3725	0.3730	0.9713	0.9253	0.9767	0.9557

Prediction with ANN

ANN model developed in this research has four neurons in the input layer and 4 neurons in the output layer as illustrated in Fig. 5. One hidden layer with 6 neurons was used in the architecture because of its minimum % error values for training and testing sets. While modeling networks, age of specimen (days), temperature (°C), type of cooling and density (g/cm^3) were used as input parameters and the engineering properties (N/mm^2) were used as output parameters.

For training set, 25 samples were selected and the residual data 5 samples were selected as testing set. The limit values of input and output variables used in the multi-layer feed-forward neural network model are listed in Table 5. The values of the training and test data were normalized between 0 and 1 using Equation 4.

$$F = (F_i - F_{min}) / (F_{max} - F_{min}) \quad (4)$$

In this equation (Serkan, 2009), F represents the normalized value, F_i represents the i^{th} measured value and F_{max} and F_{min} were used in feed-forward model with 1 hidden layer. Logarithmic sigmoid transfer function was used as the activation function for hidden and output layers. Because the back propagation network weights cannot be easily understood in the form of a numeric matrix, therefore they may be transformed into coding values in the form of a percentage by dividing the weights by the sum of all the input parameters. This gives the relative importance for each input parameter to the output parameter. The relative importance for various input parameters is shown in Fig. 6 and the major dominant parameter is the density (63.31%). Similarly, the relative importance of variables; age, temperature and cooling type are: 18.03, 11.09 and 6.76%, respectively.

Comparison of Prediction Techniques with ANN

All results obtained from experimental studies and

predicted by using the training and testing results of the ANN and RT, for compressive strength, flexural strength, splitting strength and modulus of elasticity are shown in Fig. 7. As seen in the Figure, good results were obtained from the multi-layer feed-forward neural network model. It is so obvious that mostly 98% of the data is located on the line of equality which means that the actual and the predicted values for the engineering properties of RPC are identical through the use of ANN model. This is quite true, because the correlation coefficient was about 0.98 for the prediction of properties of RPC after burning. The statistical values of RMSE, MPAE, MPA, R^2 and AA including all the stations for both training and testing for ANN and RT are given in Table 7. From the statistical values in this table, one can see that the proposed multi-layer feed-forward neural network model is suitable and predicts the compressive strength, flexural strength, splitting strength and modulus of elasticity of RPC after burning. Values became very close to the experimental values. It is stated that predictions achieved from back-propagation ANN applications showed better results than RT. It can be seen from Table 7, that the smallest prediction errors are observed in ANN technique

Table 8. Testing data sets for comparison of experimental results with testing results predicted from models

Age at Exposure (days)	Compressive strength [MPa]			Flexural strength [MPa]			Splitting strength [MPa]			Modulus of elasticity [GPa]		
	Experiment	ANN	RT	Experiment	ANN	RT	Experiment	ANN	RT	Experiment	ANN	RT
3	91.12	93.10	94.65	30.00	30.40	29.11	9.90	9.74	9.80	37.07	38.20	36.12
	100.38	102.12	106.08	39.66	39.74	38.53	12.70	12.36	12.70	39.66	40.67	39.27
	94.80	95.14	99.41	37.81	37.39	35.21	11.35	11.23	11.46	37.81	37.33	35.83
	66.69	63.13	79.09	26.32	22.04	25.32	6.63	7.23	8.84	26.32	25.31	27.30
	65.52	63.05	75.47	24.84	21.69	24.01	6.24	6.82	8.27	24.84	24.73	25.82
	61.05	55.56	62.36	23.72	20.23	18.87	6.14	6.68	7.23	23.72	24.00	21.94
	59.23	55.35	58.87	22.61	18.63	17.64	5.94	6.22	6.69	22.61	23.50	20.55
7	99.40	93.86	90.20	37.70	36.65	34.82	13.42	13.22	12.76	37.70	36.78	35.40
	123.00	116.30	109.87	42.22	41.90	39.35	14.41	14.13	13.08	42.22	41.64	40.32
	109.00	114.12	106.39	41.09	40.86	38.13	14.19	13.35	12.54	41.09	40.58	38.93
	79.02	80.71	86.63	27.52	25.31	28.60	9.25	9.35	10.04	27.52	27.35	30.76
	76.74	81.60	82.73	26.39	25.24	27.11	8.59	8.95	9.41	26.39	27.43	29.10
	72.57	73.87	70.31	25.26	23.75	22.42	8.86	8.88	8.53	25.26	26.81	25.66
	70.28	73.35	66.13	24.13	21.51	20.74	8.32	8.24	7.84	24.13	26.04	23.83
28	132.30	130.85	126.30	41.00	40.26	38.33	15.67	15.34	14.37	41.00	42.10	38.10
	143.80	141.77	130.82	47.15	47.35	44.31	16.72	16.84	15.30	47.15	48.27	46.49
	134.70	143.11	130.80	45.51	46.57	45.37	16.50	16.31	15.53	45.51	48.94	47.33
	102.22	97.50	103.00	30.75	27.85	30.56	11.59	11.19	11.26	30.75	30.18	33.99
	100.24	96.90	97.43	29.11	26.23	27.97	10.97	10.61	10.26	29.11	28.94	31.26
	91.24	93.23	86.96	29.52	26.11	24.56	11.28	10.94	9.81	29.52	30.35	29.07
	88.78	90.91	80.70	28.29	22.98	21.51	10.65	10.15	8.66	28.29	28.26	25.90
56	147.50	148.90	151.00	46.00	42.85	40.08	16.00	16.82	17.08	46.00	47.46	43.05
	157.20	163.20	157.36	54.74	49.60	50.02	17.50	18.08	17.97	54.74	55.02	53.83
	154.20	153.12	160.12	52.44	47.62	52.91	16.90	16.73	18.80	52.44	53.40	56.46
	126.99	125.22	123.85	35.88	30.12	32.53	12.48	12.47	12.67	35.88	35.53	37.67
	125.67	124.18	117.74	34.50	29.84	29.58	11.84	12.15	11.56	34.50	34.74	34.58
	112.10	115.95	111.97	34.04	27.16	29.26	11.84	11.68	12.14	34.04	35.28	35.43
	109.29	114.90	105.72	32.66	25.22	26.22	11.20	10.84	10.99	32.66	33.41	32.26
90	174.05	173.41	175.55	54.28	52.08	50.21	18.88	18.41	18.02	54.28	53.90	51.87
	185.50	185.21	185.07	64.59	56.96	53.99	20.65	20.97	20.21	64.59	62.46	59.84
	181.96	177.75	188.02	61.88	55.67	57.00	19.94	19.94	21.08	61.88	61.76	62.59
	149.85	148.86	151.09	42.34	38.12	36.18	14.73	15.58	14.81	42.34	43.45	43.37
	148.29	139.48	144.99	40.71	34.88	33.24	13.97	14.20	13.70	40.71	39.39	40.29
	132.28	133.41	139.17	40.17	33.34	32.89	13.97	13.99	14.26	40.17	41.02	41.10
	128.96	131.26	132.92	38.54	31.42	29.85	13.22	13.06	13.12	38.54	38.82	37.94

according to the performance criteria such as RMSE, MPAE, MPA, R^2 and AA. The prediction success of ANN technique was much better than that of the regression technique (RT). The best value of R^2 is 0.990 for testing set in the ANN model. The minimum value of R^2 is 0.925 for testing set in the RT model. All the results obtained from experimental studies of engineering properties of RPC values before and after exposure to fire flame and the predicted values by both techniques are presented in Table 8. It can be concluded from these results that the proposed multi-layer feed-forward neural network model is suitable and predicts compressive strength, flexural strength, splitting tensile strength and modulus of elasticity of RPC after exposure to fire flame. Values became closer to the experimental values compared with those in RT.

The relationships between the observed mechanical values and the predicted performance obtained from ANN and RT models were illustrated in Fig. 8. The Figure shows that the distribution of values is around the neutral axis and the ANN model is supported by statistical evidence more than the RT model. Figs. 9 and 10 compare the mechanical properties of RPC after exposure to fire flame of ANN, RT and the observed values of the output. The values predicated by ANN were much closer to the observed values as compared to those predicted by RT. These graphs can provide an insight into understanding the trend predicting values. However, in both the cases, ANN has a good potential for predicting exact values in comparison to RT for the same objective. Finally, we can statistically depict that the collected results from the statistical programs which were compared with the practical results improved the closeness of the ANN results to the practical results. This can be shown through the mentioned values in Table 8, then being illustrated. In addition, this can be shown through the variables prediction models in Table 7.

CONCLUSIONS

Based on the experimental results presented in this research, the following conclusions are obtained from this study:

1. The residual strength of RPC decreases with increasing temperature from 200°C.
2. High fire flame temperatures can be divided into two ranges in terms of strength loss in RPC; namely, 23-200°C and 300-500°C. In the range 23-200°C, RPC maintained or even gained an increase in the original strength. In the range 300-400°C, RPC lost original strength considerably. When burning RPC specimens at about 500°C, they spalled and lost both mechanical and physical properties with partial or total spalling.
3. Crack propagation sounds for about 4-7 minutes are recorded at the extreme test temperature. Small pieces fell out of the surface layer; while explosive spalling was recorded at around 21 minutes. After the spalling, big parts fell out. When 30 minutes were completed and the fire source was removed, the samples were found with different and non-uniform shapes and with damaged edges.
4. The study suggests the use of RPC as pre-cast concrete elements at elevated temperatures up to 400°C, taking into consideration the loss of strength by values up to about 35%. Cautiously, the use of RPC above this temperature is not a wise choice as the study shows.
5. The mechanical properties values predicted from testing the multi-layer feed-forward neural network model were much closer to the experimental results than the predicted values of the regression model and these models proved useful with any set of data in spite of variations in test results of the RPC in question.
6. The proposed mathematical and mechanical models were capable of predicting the effect of burning by real fire flame to produce the required concrete mechanical properties.
7. Results with the data set suggest that ANN-based modeling approach can effectively be used in predicting the engineering properties of RPC after exposure to fire flame.

The parametric study showed that the density is the most significant factor affecting the output of the model. On the other hand, the relative importance of values of other input parameters is insignificant with respect to the importance of density.

REFERENCES

Adhikary, B.B., and Mutsuyoshi, H. (2006). "Prediction of Shear Strength of Steel Fiber RC Beams Using Neural Networks". Constr. Build. Mater., 20 (9), 801-811.

Altun, F., Kisi, O., and Aydin, K. (2008). "Predicting the Compressive Strength of Steel Fiber Added Lightweight Concrete Using Neural Network". Computat. Mat. Sci., 42 (2), 259-265.

ASTM C 1240. "Standard Specification for the Use of Silica Fume as a Mineral Admixture in Hydraulic Cement Concrete, Mortar and Grout". 4 (2), 1.

ASTM C 496. (2005). "Standard Test Method for Splitting Tensile Strength of Cylindrical Concrete Specimens". 04.02.

ASTM C469. (20002). "Standard Test Method for Static Modulus of Elasticity and Poisson's Ratio of Concrete in Compression".

ASTM C494. (1999). "Chemical Admixture for Concrete". Annual Book of ASTM Standards American Society for Testing and Materials, 04.02, 245-252.

ASTM C78. (2002). "Standard Test Method for Flexural Strength of Hydraulic-Cement Mortars". 04.02, 6pp.

Bonneau, O., Poulin, C., Dugat, J., Richard, P., and Aitcin, P. C. (1996). "Reactive Powder Concretes: from Theory to Practice". Concrete International, 18 (4), 47-49.

B.S. 1881: Part 116. (1989). "Method of Determination of Compressive Strength of Concrete Cubes". British Standards Institution.

Chan, Y. N. S., Peng, G. F., and Anson, M. (1999). "Residual Strength and Pore Structure of High-strength Concrete and Normal Strength Concrete after Exposure to High Temperatures." Cement and Concrete Composites, 21 (1), 23-27.

Cheyrezy, M., Maret, V., and Frouin, L. (1995). "Micro-Structural Analysis of RPC (Reactive Powder Concrete)". Cement and Concrete Research, 25 (7), 1491-1500.

Hagera, I., Zdeb, T., and Krzemie´n, K. (2013). "The Impact of the Amount of Polypropylene Fibres on Spalling Behaviour and Residual Mechanical Properties of Reactive Powder Concretes". 1-8, MATEC Web of Conferences. Poland.

Hamzaçebi, C., and Kutay, F. (2005). "Determining Input and Hidden Neurons Numbers in Artificial Neural Networks for Forecasting Stationary Time Series". J. TÜ_K Stat. Res., 4, 2.

Hassan, F.H. (2012). "Punching Shear Behavior of Normal and Modified Reactive Powder Concretes Slabs". Al-Mustansiriya University, Baghdad, Iraq, PhD Thesis, Department of Civil Engineering (Structures), College of Engineering, September, 188p.

Hussein, A.A. (2011). "Punching Shear Strength of Reactive Powder Concrete Flat Plates". Al-Mustansiriya University, Baghdad, Iraq, M.Sc. Thesis, Department of Civil Engineering, College of Engineering, October, 124p.

Ince, R. (2004). "Prediction of Fracture Parameters of Concrete by Artificial Neural Networks". Eng.Fract.Mech., 71 (15), 2143-2159.

Iraqi Specification No. 45. (1984). "Aggregate from Natural Sources for Concrete and Construction". Ministry of Planning, Central Organization for Standardization and Quality Control.

Iraqi Specification No. 5. (1984). "Portland Cement". Ministry of Planning, Central Organization for Standardization and Quality Control.

Kalayci. (2006). "Multi-Varied Statistical Techniques and SPSS Applications". Ankara, Asil Publishing.

Lee, S.C. (2003). "Prediction of Concrete Strength Using Artificial Neural Networks". Eng. Structures, 25, 849-857.

Lin, C., and Lee, C.S.G. (1996). "Neural Fuzzy Systems". Prentice Hall, New Jersey.

Liu, C.T., and Huang, J.S. (2009). "Fire Performance of Highly Flowable Reactive Powder Concrete". Construction and Building Materials, 23, 2072–2079.

Ozer, M., Isik, N.S., and Orhan, M. (2008). "Statistical and Neural Network Assessment of the Compression Index of Clay Bearing Soils". Bull. Eng. Geol. Environ., 67, 537-545.

Pala, M., Ozbay, E., Oztas, A., and Yuce, M.I. (2007). "Appraisal of Long-term Effects of Fly Ash and Silica Fume on Compressive Strength of Concrete by Neural Networks". Construction and Building Materials, 21 (2), 384-394.

Phan, L.T., and Carino, N.J. (2001). "Mechanical Properties of High Strength Concrete at Elevated Temperatures". Gaithersburg, Maryland: NISTIR 6726, Building and Fire Research Laboratory, National Institute of Standards and Technology.

Ratvio, J. (2001). "Ultralujan Betonin Kayttosovellukset Esitutkimus (Preliminary Study of Ultra Strength Concrete Applications)". VTT Tiedotteita, 2078, 3-45.

Sancak, E. (2009). "Prediction of Bond Strength of Lightweight Concretes by Using Artificial Neural Networks". Sci. Res. Essay, 4 (4), 256-266.

Schneider, U., Diederichs, U., Horvath J. et al. (2003). "Verhalten von Ultrahochfesten Betonen (UHPC) unter Randbeanspruchung (Behaviour of Ultra High Performance Concrete (UHPC) under Fire Exposure)." Beton- und Stahlbetonbau, 98 (7), 408-417.

Serkan, S. (2009). "Prediction of Mechanical Properties of Cement Containing Class C Fly Ash by Using Artificial Neural Network and Regression Technique". Scientific Research and Essay, Academic Journals, 4 (4), 289-297.

Subasi, S., and Beycioglu, A. (2008). "Determining the Compressive Strength of Crushed Limestone Aggregate Concrete Using Different Prediction Methods". e-J. N. World Sci. Acad., 3 (4), 580-589.

Sujatha, T., and Basanthi, D. (2014). "Modified Reactive Powder Concrete".

International Journal of Education Applied Research (IJEAR), India.

Therresa, M., Erron, A., and Donald, M. (2008). "Ultra High-Performance Concrete for Michigan Bridges Material Performance Phase-I, Center for Structural Durability". Michigan Technological Transpiration Institute, Final Report-November, 152.

Topcu, I.B., and Saridemir, M. (2008). "Prediction of Compressive Strength of Concrete Containing Fly Ash Using Artificial Neural Network and Fuzzy Logic". Computat. Mat. Sci., 41 (3), 305-311.

Toumi, B., Resheidat, M., Guemmadi, Z. and Chabi, H. (2009). "Coupled Effect of High Temperature and Heating Time on the Residual Strength of Normal and High-Strength Concretes". Jordan Journal of Civil Eng., 3 (4), 322-330.

Zhang, G., Patuwo, B.E., and Hu, M.Y. (1998). "Forecasting with Artificial Neural Networks: State of the Art., Int. J. Forecasting, 14, 35-62.